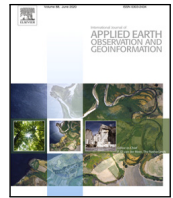




Contents lists available at ScienceDirect

International Journal of Applied Earth Observation and Geoinformation

journal homepage: www.elsevier.com/locate/jag

Cloud-based interactive susceptibility modeling of gully erosion in Google Earth Engine

Giacomo Titti ^{a,b}, Gabriele Nicola Napoli ^c, Christian Conoscenti ^c, Luigi Lombardo ^{d,*}^a Department of Civil, Chemical, Environmental and Materials Engineering, Alma Mater Studiorum University of Bologna, Viale Risorgimento, 2, 40136 Bologna, Italy^b Research Institute for Geo-Hydrological Protection, Italian National Research Council, C.so Stati Uniti, 4, 35127 Padova, Italy^c University of Palermo, Department of Earth and Marine Sciences, Via Archirafi 22, 90123 Palermo, Italy^d University of Twente, Faculty of Geo-Information Science and Earth Observation (ITC), PO Box 217, Enschede, AE 7500, Netherlands

ARTICLE INFO

Dataset link: <https://github.com/giactitti/STGEE>

Keywords:

Susceptibility modeling
Google Earth Engine
Cloud computing
Open sourcing

ABSTRACT

The gully erosion susceptibility literature is largely dominated by contributions focused on model comparison. This has led to prioritize certain aspects and leave others underdeveloped as compared to other natural hazard applications. For instance, in gully erosion data-driven modeling most studies use different platforms when it comes to data management, modeling and conversion into predictive maps. This in turn has limited the scope to catchment-scales. In this manuscript, we opt to propose a tool where the whole modeling procedure is unified within the same cloud computing system, allowing one to get rid of potential errors caused by input/output operations but also to extend the study areas indefinitely, as cloud data-management tools easily offer access to global data. Specifically, we present an interactive tool for susceptibility modeling in Google Earth Engine (GEE), the Susceptibility Tool for GEE (STGEE). Our tool requires few input data and makes use of the breadth of predictors' information available in GEE. In this cloud computing environment, binary classifiers typical of susceptibility models can be called and fed with information related to mapping units and any natural hazards' distribution over the geographic space. We tested our tool to generate susceptibility estimates for gully erosion occurrences in a study area located in Sicily (Italy). The tool we propose is equipped with a series of functions to aggregate the predictors' information in space and time over a mapping unit of choice. Here we chose a Slope Unit partition but any polygonal structure can be chosen by the user. Once this information is derived, our tool calls for a Random Forest classifier to distinguish locations prone to gully erosion from locations where this process is not probabilistically expected to develop. This is done while providing a modeling performance overview, accessible via a separate panel. Such performance can be calculated on the basis of an exploratory analysis where all the information is used to fit a benchmark model as well as a spatial k-fold cross-validation scheme. Ultimately, the predictive function can be interactively used to generate susceptibility maps in real time, for the study area as well as any study area of interest. To promote the use of our tool, we are sharing it in a GitHub repository accessible at this link: <https://github.com/giactitti/STGEE>.

1. Introduction

Planning actions aimed at reducing or mitigating disaster risk share a common starting point irrespective of the natural hazard under consideration. This starting point assumes that we can estimate where, how frequently and how threatening a given natural process may be (Klügel, 2008; Domeneghetti et al., 2013; Lombardo et al., 2020a). Estimating these three elements in the future constitutes an attempt to predict natural hazard occurrences and associated characteristics, so that decisions can be made to alleviate the risk. For instance, investments can be made to stabilize a potentially unstable slope (Abramson et al., 2001) or

flood barriers can be built to limit the water invasion of lands outside the river bed (Srb et al., 2017), and so on for other type of hazard. Predicting the locations where natural hazards may occur is commonly referred to as susceptibility. The evolution of susceptibility models has substantially evolved in the last four decades. From expert-based notes taken on a paper (see, Brabb et al., 1972), the geoscientific community has initially moved to knowledge-driven models (e.g., Leoni et al., 2009) where some of the operations were carried out in a digital platform but still based on the subjective judgement of the person behind the assessment. Then the data-driven framework took over the scene,

* Corresponding author.

E-mail address: l.lombardo@utwente.nl (L. Lombardo).

initially in a bivariate context (e.g., [Nandi and Shakoor, 2010](#)), quickly superseded by its multivariate counterpart (e.g., [Lombardo and Mai, 2018](#); [Titti et al., 2021](#)). Even more recently, machine learning tools have provided equally valid alternatives to the multivariate statistical tools, bringing more in terms of performance, losing though in terms of interpretation ([Goetz et al., 2011](#)). Despite this rapid evolution, something has never changed. Irrespective of the user's technical ability, the most common analytical protocol includes an initial phase where data is collected from many different cartographic sources. This information is then locally managed in a GIS platform where it is exported to be used in a computing environment such as Matlab (e.g., [Lagomarsino et al., 2017](#)), R (e.g., [Brenning, 2008](#)) or Python ([Gerzsenyi, 2021](#)). These computing environments allow for different models to be run, for the susceptibility to be estimated and to export the results back into a GIS where the results are ultimately converted in map form. Very few cases exist where these long series of cross-platform input/output operations are kept within the same environment, e.g., [Bragagnolo et al. \(2020\)](#) within GRASS GIS and [Naghbi et al. \(2021\)](#) within ArcGIS. But, even in these cases, the computing phase of the research takes place on local machines and the potential of cloud computing resources has yet to be tapped in. In fact, the very recent birth and evolution of cloud-based systems have enabled scientists and end users in general to perform data management and computing procedures all within the same environment. This mostly constitutes an uncharted territory also for the natural hazard community, although cloud solution hold a great potential for scientist to unify their data access and modeling protocols within the same remote environment. In this sense, a very small number of articles proposes to use a web-based platform such as Google Earth Engine (GEE, hereafter). [Najafi et al. \(2020\)](#) uses GEE to extract the predictor set for land subsidence assessment in a Iranian study site, but then the authors perform the modeling operations in their local machine. [Scheip and Wegmann \(2021\)](#) exploit GEE to automatically map multiple hazards on the basis of time series of normalized difference vegetation index (NDVI) data. [Ilmy et al. \(2021\)](#) manage the predictor set in their local machine, built a landslide susceptibility into GEE only to export the data back to their computers where they then translated the output into maps. This research takes inspiration from these articles but largely improve on their implementation side by providing a unique environment for data handling, predictor's extraction, model building and susceptibility mapping. The only pre-requirement, is the definition of a spatial partition and the assignment of a presence/absence label to each of the mapping units.

The aim of this research is to test whether it is possible to unify modeling practices (data acquisition, preprocessing, modeling, and map making) that have been traditionally conducted in a separate manner. And, to unify this protocol in a cloud computing environment where model transferability becomes an easy task due to data availability. Therefore, we present the Susceptibility Tool for Google Earth Engine (STGEE).

The following sections are meant to elucidate the tool we propose, by describing its sub-routines while taking the generation of gully erosion susceptibility as an example. More specifically, Section 2.1 introduces the study area and the gullies we mapped. Section 2.2 describes the spatial partition we opted for. Then Section 2.3 dives into GEE for the extraction of the predictor set and Section 3 expands on that to illustrate the use of a binary classifier directly within GEE. As a result, the tool will perform the model building phase, calculation of performance metrics and cross-validation routines. The interactive visualization will also be explained. The results are then presented in Section 4, and the strengths of the tool we propose are then discussed in Section 5. We conclude the paper in Section 6 where we share with the readers our vision for the next directions to take when aiming at estimating natural hazard occurrences in a cloud-based environment.

2. Data overview

2.1. Study area and gully inventory

The study area is part of the Belice catchment, located in the western part of Sicily facing the Mediterranean Sea to the South-West (see [Fig. 1Zoom1](#)). The area where we test our tool is shown in [Fig. 1Zoom2](#) and extends for approximately 77 km² with a maximum length of around 17 km. Hydrologically, it consists of a tributary of the Belice catchment. As for the climate conditions the area is exposed to, a typical Mediterranean climate regime controls hot and almost dry summers, alternated to wet and warm autumn–winters (more details provided in [Conoscenti et al. \(2015\)](#)).

For what concerns the precipitation trends, a mean annual discharge of around 50 mm is associated with a mean annual temperature of 30 C°. According to WorldClim database ([Hijmans et al., 2005](#)), most rainfall is discharged in the months of October (77 mm), November (75 mm) and December (75 mm). During these months, the area is affected by a wide range of water erosion and land degradation phenomena due to the widespread presence of fine-grained deposits and intensive agriculture. Specifically, field evidence has shown saturation of these deposits during heavy rain, initially resulting in loss of cohesion and then in surface deformation and formation of gullies [Conoscenti et al. \(2015\)](#). Most of the gullies occur on cultivated fields and can be classified as ephemeral. The gully channels indeed are usually erased by tillage operations a few months after their formation. [Fig. 1Zoom3](#) shows instead a nearby catchment we chose to purely demonstrate the spatial transferability of our modeling framework.

2.2. Mapping unit

Our tool works irrespective of the mapping unit one would like to use. As the choice of the mapping unit is strictly connected to the hazard one needs to model, our choice to test our tool for gully erosion susceptibility implies that the specific mapping unit would have respected the hydro-morphological behavior of this type of hazard or that at least, it would have been justified from past literature. The literature on gully erosion susceptibility reports a large number of contributions where a regular grid is preferred (e.g., [Cama et al., 2020](#)), followed by fewer examples on Unique Condition Units (e.g., [Conoscenti et al., 2013](#)) and Slope Units (e.g., [Lombardo et al., 2020b](#)). Here we opted for the latter case, having generated our Slope Unit (SU) partition through *r.watershed* in GRASS GIS ([Neteler and Mitasova, 2013](#)). As a result, our study area has been divided into 1000 SU, with a mean planimetric area of 0.066 km² and a standard deviation of their extent equal to 0.042 km².

2.3. Predictors

Our predictor choice exploits the breadth of information contained in GEE. There, terrain, climatic, vegetation characteristics can be easily accessed. However, the resolution at which this information is expressed may significantly differ from the resolution of the mapping unit one may want to use. The most common situation for natural hazards is that the scale at which these processes act and develop is larger than the dimension at which most remote sensing data is collected. For instance, elevation data can be globally found at a 30 m resolution and yet landslides may be much wider or longer than a single 30 × 30 grid cell. The same is evident for floods and wildfires, two process that may affect large portions of a territory. As a result, the choice of an appropriate mapping unit should reflect the dimensionality of the process under consideration. For geomorphological processes this usually results in medium resolution objects such as slope units ([Carrara, 1988](#); [Bryce et al., 2022](#)) or catchments ([Wang et al., 2021, 2022](#)).

As a result of the considerations above, one may find that a large number of grid-cells falls within a single mapping unit. And, for the

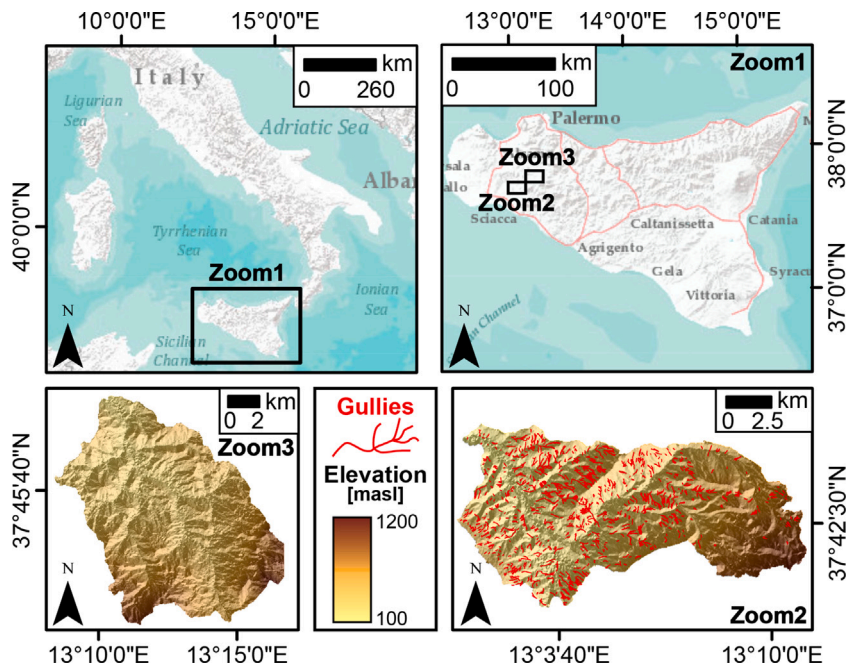


Fig. 1. Left to right: Geographic overview; Location of the test site (Zoom2) and the prediction target (Zoom3, see at the end of Section 3); Zoom2 shows the gullies we inventoried to test our tool together with the underlying topography.

Table 1
Predisposing and triggering factors (see Titti et al., 2022, for an example).

	Data type	Data source	Layer	Acronym
1	Morphology	SRTM (Farr et al., 2007)	Slope degree mean	S_mean
2			Slope degree std	S_std
3			Plan curvature mean	HCv_mean
4			Plan curvature std	HCv_std
5			Profile curvature mean	VCv_mean
6			Profile curvature std	VCv_std
7	Precipitation	CHIRPS (Funk et al., 2015)	Annual precipitation mean	Prec_mean
8			Annual precipitation std	Prec_std
9	NDVI/NDWI	Copernicus Sentinel data 2015–2020	NDVI mean	NDVI_mean
10			NDVI std	NDVI_std
11			NDWI mean	NDWI_mean
12			NDWI std	NDWI_std

specific example of SUs, even thousand if not millions of grid-cells may be contained in a single polygon. Therefore, the resulting distribution per SU needs to be summarized according to fewer statistical moments such as the mean and standard deviation (Guzzetti et al., 2005) or according to a richer quantile description (Castro Camilo et al., 2017). Here we have chosen to use the mean and standard deviation values, having prepared another set of function in GEE to complete this task. These functions are part of another GEE tool we have previously built, called Spatial Reduction Tool (SRT, Titti and Lombardo, 2022) and accessible at this link. More specifically, SRT allows one to compute terrain attributes from globally available DEMs directly within GEE, as well as other upscaling operations for climatic, temperature and vegetation data, which are commonly expressed both in space and time. In Table 1 we report the predictors we extracted for this study.

In Section 4, additional details will be provided to explain how to select the predictor set through our tool and how to create the data matrix required model. Here we conclude mentioning that we label each slope unit according to the presence or absence of gullies by checking the intersection between the two. All the slope units that intersect gullies are assigned with a presence label whereas the opposite situation defines the absence case.

3. Model building strategy

We have chosen a Random Forest (RF; see Biau and Scornet, 2016, for modeling details) classifier among the available ones in GEE. We have done so because the general family of decision trees has a long history of successful applications in the susceptibility literature (e.g., Lombardo et al., 2015; Hong et al., 2020) and specifically RF has proven to be a valid modeling framework when modeling different types of natural hazards, from wildfires (Tonini et al., 2020) to landslides (Taalab et al., 2018) and specifically in the context of gully erosion (Avand et al., 2019).

A RF is undoubtedly a powerful tool for any binary classification tasks, but still requires its modeling performance to be estimated and summarized across a series of tests. We chose to assess the classification performance via Receiver Operating Characteristic curves and their Area Under the Curve (Rahmati et al., 2019). Our tool integrates a ROC function into the whole modeling protocol and graphically returns ROC curve, AUC and best probability cutoff as part of the GEE plotting space. Our tool supports the use of performance estimations in two steps. The first step computes the goodness-of-fit performance, testing the agreement between observed and fitted presence/absence data. As for the actual predictive performance, being the data we used purely

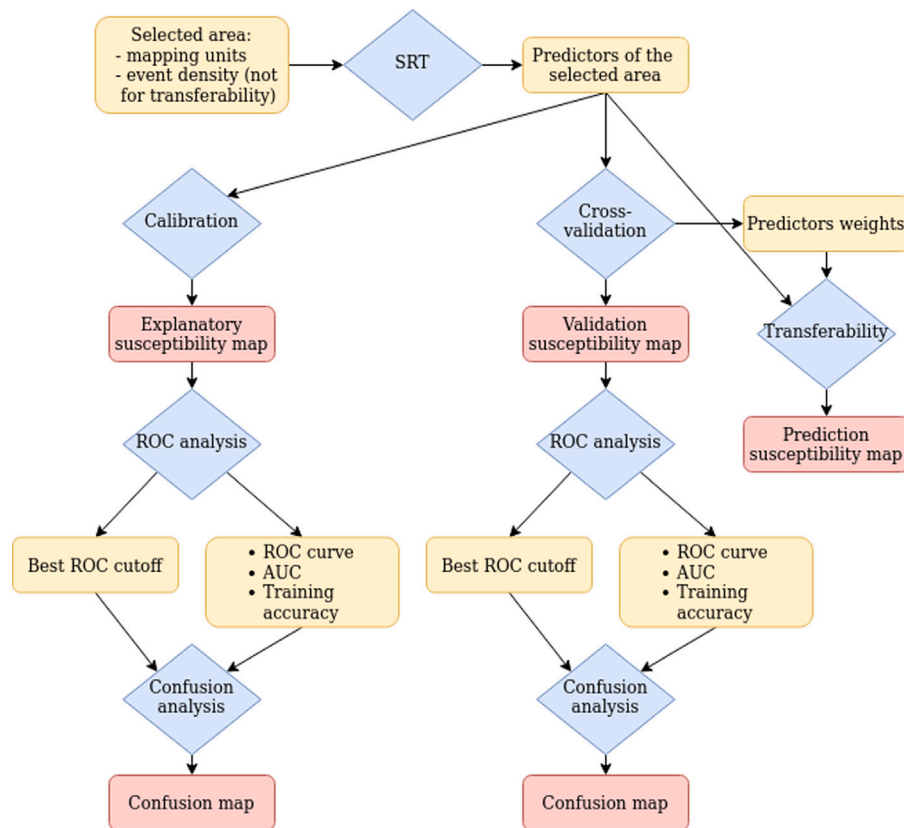


Fig. 2. Flow-chart of the main steps and functions used by the STGEE.

spatial, we adopted a spatial cross-validation scheme (SCV; see Steger et al., 2016). We could have opted for a purely random cross-validation but these operations tend to keep the modeling performance quite close to the actual calibration because they retain the spatial structure in the data and an elegant explanation on the topic can be found in Schratz et al. (2019). For this reason, we opted to implement a SCV, as it ensures that any residual spatial structure in the data is disentangled from the performance assessment. In our tool, we offer to the user the chance to select the dimension of a squared lattice, whose structure is used for the SCV. This implies that every mapping unit falling within a grid of the lattice will be iteratively kept aside for testing and the complementary mapping units will be used for calibration. This operation is looped until all the mapping units constituting the whole study area are fully predicted.

Ultimately, we also implemented a separate tool that allows one to export the predictive function in any other area. This operation is commonly known as model transferability (Lombardo et al., 2014) and here we ensure its application within the same GEE environment as long as the user uploads the same type of spatial partition used for calibration and as long as the transferability makes sense in terms of geographic settings.

The entire workflow of the STGEE functions is shown in Fig. 2. The red squares represent the maps visible into the tool map.

Every outcome of the modeling procedure described in the previous section can be interactively visualized in GEE. We offered a series of visualization techniques to quickly explore the results. Specifically, one can plot:

- Fitted susceptibility map;
- Confusion matrix map (TP, TN, FP and FN), where the cutoff is set to the best probability cutoff computed during the ROC calculation;
- Spatially cross-validated susceptibility map;
- Spatially transferred susceptibility map.

4. Tool overview through example results

The STGEE tool is available in [GitHub](#). The repository is composed by 5 scripts: ROC, SCV, STGEE, display, run.

The STGEE tool can be ran using the “STGEE” script available at this [link](#). This code allows the user to select the input variables to be used in the susceptibility model. Four inputs are necessary to launch all the functions of the STGEE: “predictors_shp” a vector file containing the presence/absence status and the mean and standard deviation of the predictors per mapping units; “binomial_event” the name of the attribute which reports the binomial labels of the event; “predictors_column_name” the name of the predictor attributes; and “prediction_area_shp” a vector file containing the predictors per mapping units of the predicting area. The “predictors_shp”, the “binomial_event” and the “predictors_column_name” are mandatory, the “prediction_area_shp” is only required to apply the model transferability function.

In this example, we chose a SU partition, whose gully erosion binary label corresponds to 1 for SUs containing at least one gully, and a label of 0 for gully-free SUs. The predisposing factors we used, have been collected with the SRT tool. The loading example is illustrated in Fig. 3. There, the top right drop-down panel highlighted in red allows to interactively visualize the Slope Unit partition (denominated as Study area). And, the button highlighted in blue at the center of the screen allows one to run the whole script.

Once the user clicks on the “Run analysis” button, our tools automatically selects the required predictors listed in Section 2.3 and it calls the random forest function to calibrate our initial susceptibility model. The relative output can also be interactively visualized, which we show here in Fig. 4. The figure highlights few elements in our tool that will be clarified below. First of all, in red we have highlighted again the visualization drop-down list, where we have selected the calibrated RF model. By flagging the “Calibrated map”, the susceptibility is plotted at

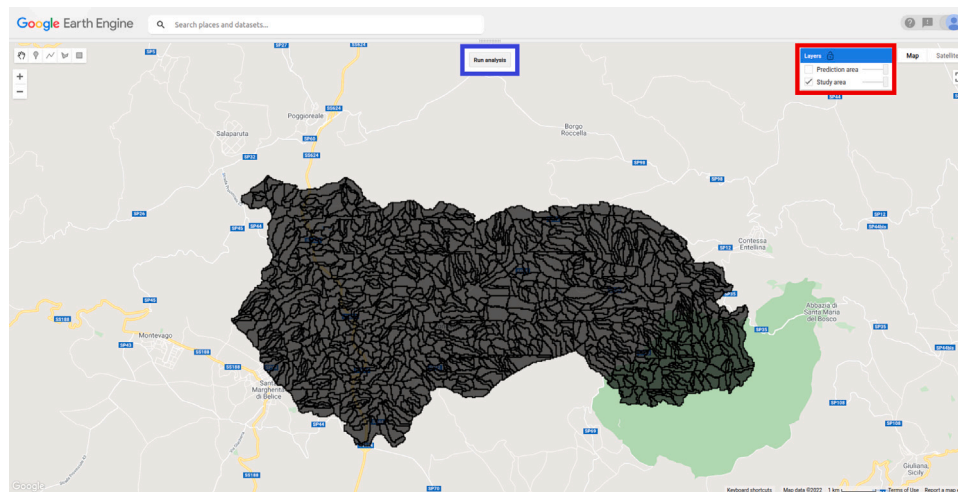


Fig. 3. Mapping unit partition overview by Google Earth Engine platform. This corresponds to the mapping unit where the model will be calibrated and validated.

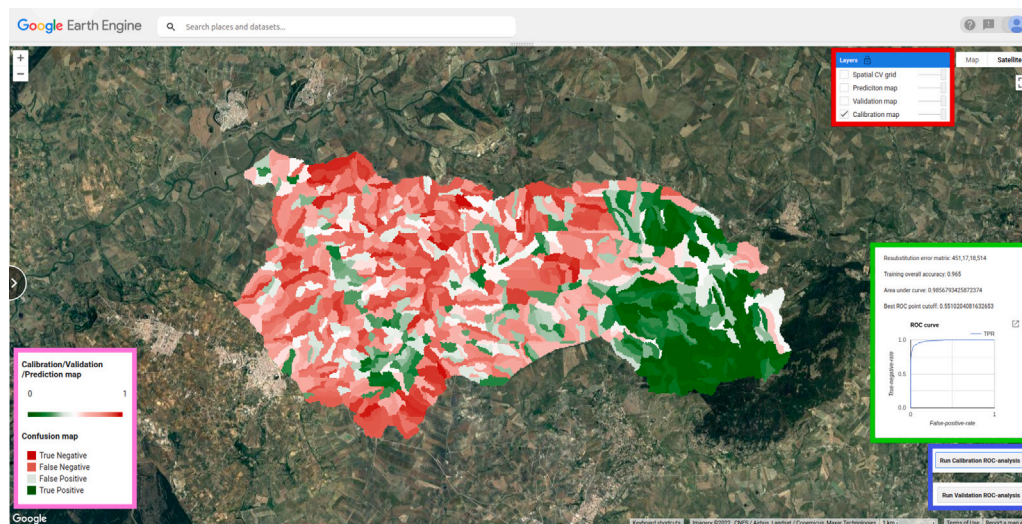


Fig. 4. Calibrated susceptibility map overview. Performance metrics are visible in the right side of the webpage. Notably, using a best probability cutoff at 0.551, the confusion matrix lists 451 True Negatives, 17 False Positives, 18 False Negatives, 514 True Positives.

the center of the screen. We have chosen a color scheme from green to red passing through white visible in the left side of the screen. Here we are showing the probabilistic results in a continuous spectrum from 0 to 1. Conversely, the second colorbar within the purple box corresponds to a visualization tool that will be described later.

The tool also offers two options: “Run calibration ROC analysis” and “Run validation ROC analysis”, shown in the panel highlighted in blue in Fig. 4. There, we have used the first option, whose performance results are summarized in the panel highlighted in green. The ROC curve related to the calibration analysis is plotted and four particularly relevant metrics are reported: the confusion matrix, accuracy, AUC and the best susceptibility cutoff to convert the continuous spectrum of probability values into discrete instances of expected gully presences and absences. The same applies to the second button “Run validation ROC analysis”, but in the case of the validation map.

In fact, a calibrated RF is a good general reference of susceptibility but it only provides goodness-of-fit performance indications, unsuited to support decision making processes. This is because the model knows all the data that it tries to estimate and thus the result cannot be considered from a predictive standpoint. Therefore, we have equipped our tool with an automated cross-validation scheme. Specifically, the cross-validation we pursue corresponds to a spatially-constrained cross-validation. This is quite known in the literature and it is well described

in articles such as (Goetz et al., 2015; Lin et al., 2021). The application of such validation routines is considered a must, especially when the mapping unit is defined at high resolution and therefore, a purely random cross-validation may reflect some auto-correlation issue from a replicate to another. Conversely, a spatial cross-validation ensures that any spatial structure in the data is disaggregated and thus would not influence the predictive performance. To allow our tool to be as generalizable as possible (in the context of small or large mapping units), we have therefore opted to implement and offer a spatial cross-validation to the user. Specifically, the way this operates in our tool is for the user to initially define a large lattice, such as the one shown in Fig. 5. This is the only operation where the user is asked to parameterize our tool. In fact, it is up to the user whether to choose for a fine or coarse lattice, although we suggest the coarse choice. Then our tool will intersect all the mapping unit falling in one of the lattice grid cells and preserve this data purely for validation purposes. In other words, the RF model will be calibrated on the remaining grids and it will iteratively move from a grid to another, exclusively storing the predicted probabilities for the mapping units under examination during the corresponding step of the loop.

The result of the spatial cross-validation can then be visualized using the same interactive structure shown in the previous figures. This is visible in Fig. 6a. But, in addition to a standard visualization,

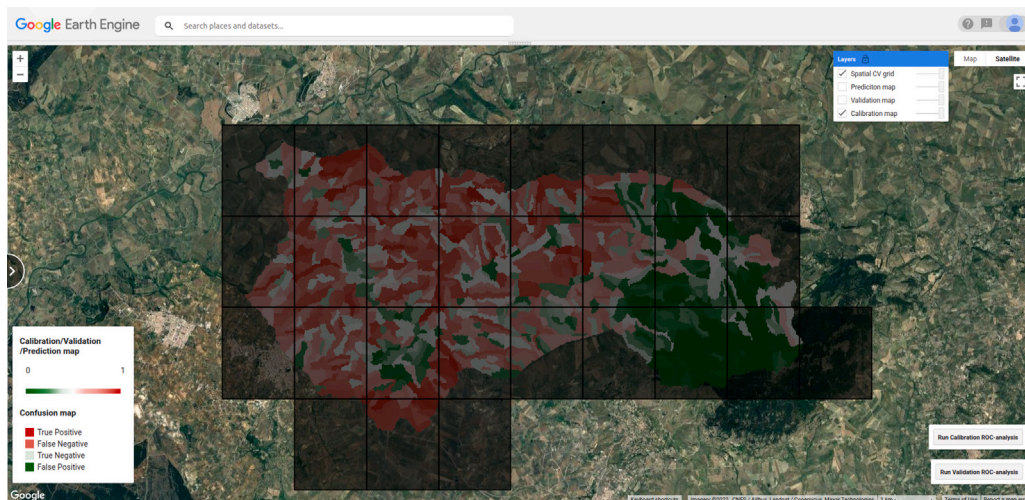


Fig. 5. Lattice generated directly in GEE to support spatial cross-validation routines.

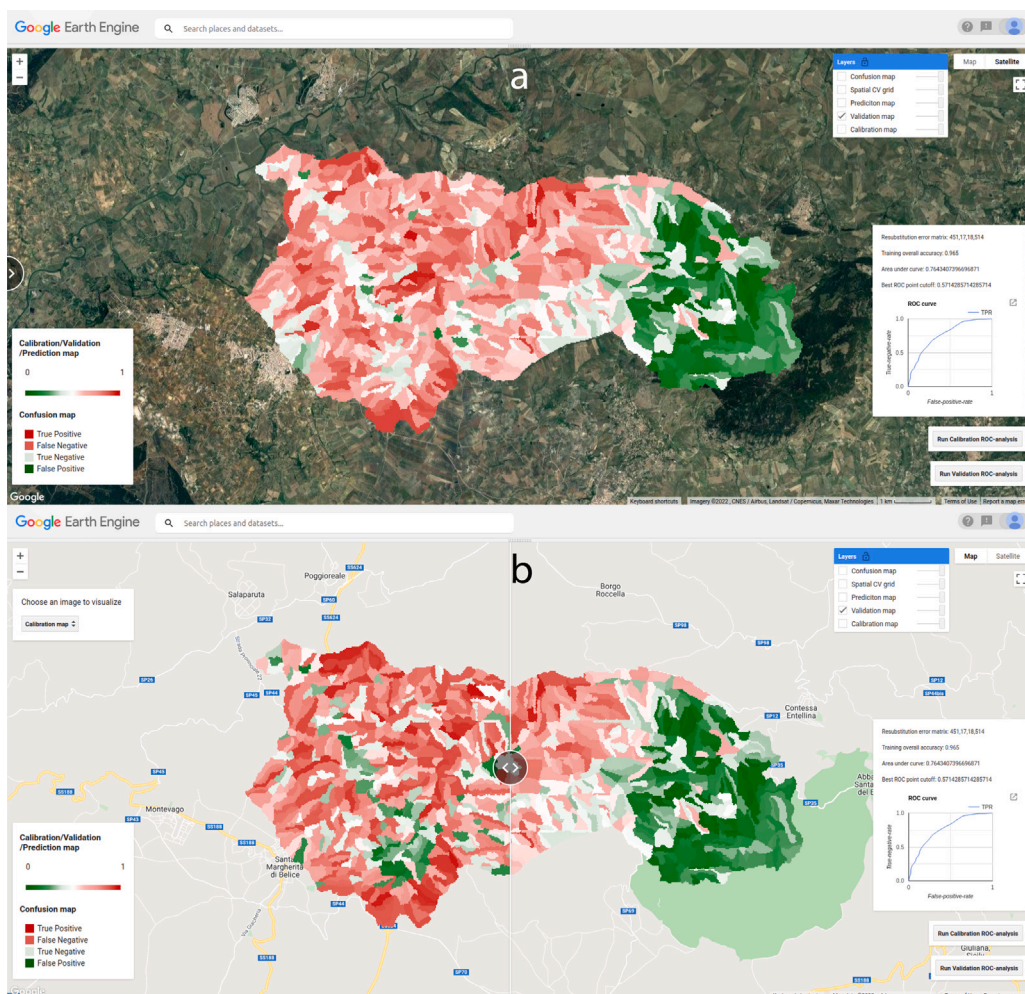


Fig. 6. Panel a: Spatially cross-validated map overview; panel b: Calibrated (left) VS spatially cross-validated (right) comparison tool. The discrete colorbar does not apply to these figures. Notably, using a best probability cutoff at 0.571, the confusion matrix lists 451 True Negatives, 17 False Positives, 18 False Negatives, 514 True Positives.

our tool supports even more interpretative considerations for the user. Specifically, we have equipped our tool with a split screen where cross-validation results can be visualized to the right and the corresponding calibrated results (same as those reported in Fig. 4) are anchored to the left side of the screen (Fig. 6b). Even in this case, one can

run performance assessment analyses and print the results on the screen for the ROC curve related metrics, including the best probability cutoff.

The aforementioned cutoff can be used to create a confusion map, i.e., the spatial distribution of TP, TN, FP and FN. Our tool also allows

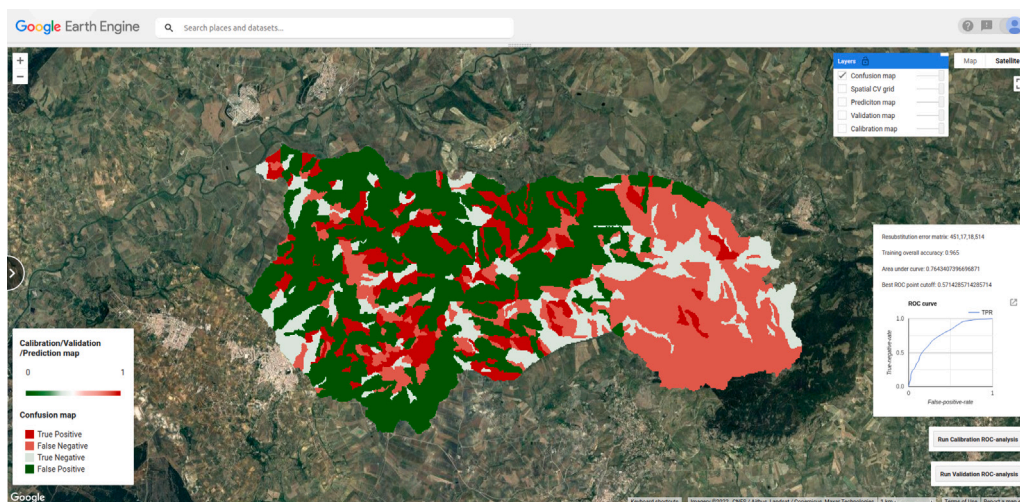


Fig. 7. Confusion map showing the spatial distribution of TP, TN, FP and FN. The colorbar that applies to this figures is the second one with four discrete classes.

one to visualize the confusion map as shown in Fig. 7. This is a particularly useful tool for potential users because it enables considerations on locations where the model hits or misses. In other words, if the FP and FN are clusters in certain regions, then there may be some unaccounted effects that need to be further explored before considering the results satisfying. Or at least, one can accept the model output as is, knowing that the estimation in certain locations is less reliable.

But, although the spatial-cross validation allows one to depict the predictive results in areas not strictly part of the calibration phase, the overall procedure is meant for validation. In other words, the predicted susceptibilities are estimated within the same area where we have information of the natural hazard at hand. In our vision of our tool, we thought of giving the user additional capabilities. In fact, once the model has been deemed suitable to estimate the susceptibility of the natural hazard one may want to study, the user can opt to extrapolate the prediction in other areas. This procedure is commonly referred to as model transferability (see, Chung and Fabbri, 2003; Lombardo et al., 2014; Cama et al., 2017) and GEE is a platform where transferability is made simple because the predictors are omni-present across the whole globe. Thus, our tool also allows to load the spatial partition of a target area and instantly transfer the predictive function there. It is important to note that not all models are transferable. For instance, one should not be able to train a landslide susceptibility model for rockfalls (Copons and Vilaplana, 2008) in mid-latitude contexts and then transfer the predictive function for thermo-karst landslides in the arctic (Nicu et al., 2021). Not only this, the appropriate spatial partition needs to be carefully considered. One cannot calibrate a model over a SU partition and then transfer it in another area on the basis of a grid cell. Therefore, it is entirely up to the user making the right choices on the validity domain of the given model transferability. This being said, in a similar manner to the initial step, the user can load the mapping unit partition of a target study area. This is shown in Fig. 8, where we have computed another SU partition (referred to as “Prediction area”) for an catchment closely located to the initial study area.

The results are shown in Fig. 9, where the estimated probability can be interactively plotted and queried, enabling considerations on master planing in areas different from those where we have collected the natural hazard inventory.

5. Discussion

Our tool makes it possible to run a RF-based classifier for susceptibility mapping directly within GEE in short time, even for relatively large datasets. Such feat is accomplished by exploiting the large computing capacity of GEE but also the functions available within GEE.

Our tool is a collection of these functions and some additional processing steps we have written using the Java Script console.

The tool is equipped with a fully functional analytical protocol that encompasses: (i) I/O functions; (ii) preprocess with the SRT for the predictors' extraction and aggregation at the scale of the chosen mapping unit; (iii) RF classification split into calibration and spatial cross-validation; (iv) performance metric estimators; (v) spatial transferability and (vi) interactive visualization.

Our tool makes it possible for any user to quickly generate probabilistic estimates across the globe and for any spatial process that can be expressed with a dichotomous label. This is an uncharted territory so far, because almost five decades of scientific development has never offered a unique platform for susceptibility modeling. So far, each scientific contribution has had to jump from a computing environment to another, with all the issues that this protocol may bring. One that comes to mind is the data formatted in different ways. Let us think about how different GIS environments encode Not-a-Number for raster data, most of the time this is encoded as -99999, but often one can find -9999 or other extremely large negative values. Therefore, when handling different predictors collected from different sources, the additional issue is to also standardize the information they carry. These problems are inherently removed when working within the same environment and our tool allows exactly for this. Another common issue is the memory management. As data has become richer and richer, datasets have become proportionally larger. The same has happened from the modeling side. As methods have become more and more complex, the computing requirements have followed the trend, making it so that the combination of big data and complex modeling routines requires dedicated computing facilities, well beyond the capacity of personal computers or laptop. This adds another level of I/O tedious practices, which our tool completely disregard. With the exception of the initial spatial partition, everything is handled within GEE. There, the specifics are obviously suitable for any model to be run, thus covering the computational aspects. As GEE capabilities and products will improve with time, we also envision a lesser need to externally manage the initial mapping units. For instance, for a catchment partition and a model built for large geographic sectors, one may use available watersheds within GEE, thus removing the need to generate the catchment vector files elsewhere. The same development may cover the aspects related to the hazard at hand. For instance, wildfire inventories can already be generated within GEE (e.g., Seydi et al., 2021). Automated landslides mapping have just started a similar journey (Scheip and Wegmann, 2021) and automated flood mapping (James et al., 2021) will soon follow. So, soon most of the operations could actually take place within cloud systems and within GEE specifically. This will guarantee an

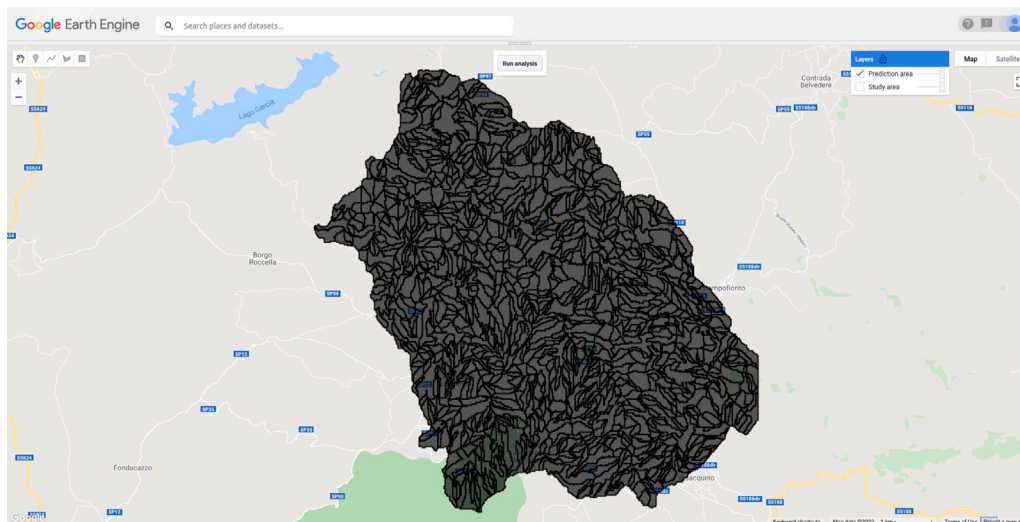


Fig. 8. Target area for model transferability, shown with the corresponding spatial partition.

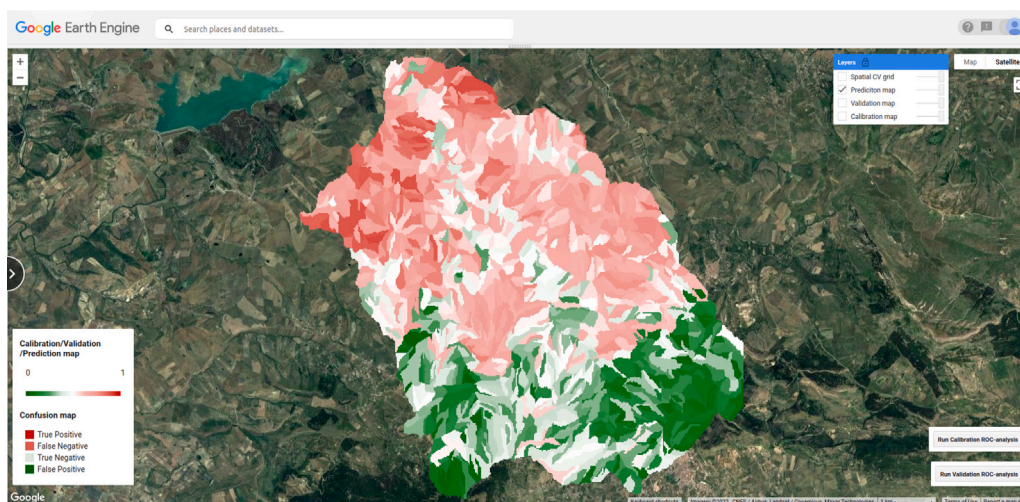


Fig. 9. Example of a transferred predictive function to another study area. We recall that the colorbar that applies to this figure is the one reporting the continuous probability values.

unprecedented level of operational capabilities, where the scientific community will get closer and closer to a unified system for natural hazard probabilistic assessment.

6. Concluding remarks

The versatility of GEE in data handling constitutes the main strength of the tool we propose. We already envision three future extensions of our tool. One is to implement different classifiers. Each model brings some level of bias in the output because of its algorithmic architecture. Conversely, different classifiers would enable ensemble modeling routines, where the combination of different approaches would average out the biases and strengthen the actual predictive signal.

The second direction we envision for our tool in the next development phase is to offer the chance to leave the binary context we have tested here, and enrich our tool with estimators for different types of data. For instance, a susceptibility framework merely inform the user of locations where a given process is more likely to occur. However, this leave unresolved the question on how many hazardous processes are expected at a given location (Lombardo et al., 2018) and how large these processes may be (Lombardo et al., 2021). In such a way, our tool could offer a full probabilistic description of natural hazards, from

their genesis to their development and help decision makers found their decisions on maps that can be essentially generated in real time. This is the third venue we are planning to pursue. In fact, the orbital frequency of modern satellites has become so frequent that the information gets streamlined on GEE almost in near-real-time or at least with such a small delay that some of the provided information can still be useful right after a major disaster. Our tool could feature static predictors (time-invariant) as well as dynamic (time-variant) ones, making it possible to generate predictive maps that change as a function of new layers uploaded within GEE.

These are research elements that are yet to be delved into within the natural hazard community, yet their importance becomes even more significant for the implementation of forecasting or early warning systems. Notably, at this stage the model we present addresses a static purely confined to the spatial case. However, we already envision a next phase in which, upon accessing gully erosion data or any other natural hazard data with a temporal connotation (date and time, in addition to the occurrence location), our tool will also be extended to solve spatio-temporal data analytic tasks, enabling early warnings to communities under potential threat.

Overall, we believe this to be just the beginning of a scientific journey where complex models can become readily available and even

easily generated by a large part of the scientific community if not to the public as a whole, thus helping the knowledge transfer and the decision making process in disaster risk management.

We shared our tool through GitHub in the hope to promote its use. The repository can be accessed at this link: <https://github.com/giactitti/STGEE>.

CRedit authorship contribution statement

Giacomo Titti: Conceptualization, Methodology, Writing – original draft, Visualization, Validation, Writing – review and editing, Software. **Gabriele Nicola Napoli:** Software, Data acquisition and curation. **Christian Conoscenti:** Data acquisition and curation. **Luigi Lombardo:** Conceptualization, Methodology, Writing – original draft, Visualization, Validation, Writing – review and editing.

Declaration of competing interest

The authors declare that they have no known competing financial interests or personal relationships that could have appeared to influence the work reported in this paper.

Data availability

Everything has been shared with the readers. Data and codes are available at this link: <https://github.com/giactitti/STGEE>; the link to the google earth engine tool is in the manuscript.

References

- Abramson, L.W., Lee, T.S., Sharma, S., Boyce, G.M., 2001. Slope stability and stabilization methods. John Wiley & Sons.
- Avand, M., Janizadeh, S., Naghibi, S.A., Pourghasemi, H.R., Khosrobeigi Bozchaloei, S., Blaschke, T., 2019. A comparative assessment of random forest and k-nearest neighbor classifiers for gully erosion susceptibility mapping. *Water* 11 (10), 2076.
- Biau, G., Scornet, E., 2016. A random forest guided tour. *Test* 25 (2), 197–227.
- Brabb, E., Pampeyan, H., Bonilla, M., 1972. MG 1972. Landslide susceptibility in San Mateo county, California. In: US Geological Survey Miscellaneous Field Studies Map MF-360, Scale, Vol. 1. (62,500).
- Bragagnolo, L., da Silva, R.V., Grzybowski, J.M.V., 2020. Landslide susceptibility mapping with r Landslide: A free open-source GIS-integrated tool based on artificial neural networks. *Environ. Model. Softw.* 123, 104565.
- Brenning, A., 2008. Statistical geocomputing combining r and SAGA: The example of landslide susceptibility analysis with generalized additive models. In: *Hamburger BeitrÄge Zur Physischen Geographie Und LandschaftsÖkologie*, Vol. 19. (23–32), p. 410.
- Bryce, E., Lombardo, L., van Westen, C., Tanyas, H., Castro-Camilo, D., 2022. Unified landslide hazard assessment using hurdle models: a case study in the island of dominica. *Stoch. Environ. Res. Risk Assess.* 1–14.
- Cama, M., Lombardo, L., Conoscenti, C., Rotigliano, E., 2017. Improving transferability strategies for debris flow susceptibility assessment: Application to the Saponara and Itala catchments (Messina, Italy). *Geomorphology* 288, 52–65.
- Cama, M., Schillaci, C., Kropáček, J., Hochschild, V., Bosino, A., Märker, M., 2020. A probabilistic assessment of soil erosion susceptibility in a head catchment of the Jemma basin, Ethiopian highlands. *Geosciences* 10 (7), 248.
- Carrara, A., 1988. Drainage and divide networks derived from high-fidelity digital terrain models. In: *Quantitative Analysis of Mineral and Energy Resources*. Springer, pp. 581–597.
- Castro Camilo, D., Lombardo, L., Mai, P., Dou, J., Huser, R., 2017. Handling high predictor dimensionality in slope-unit-based landslide susceptibility models through LASSO-penalized generalized linear model. *Environ. Model. Softw.* 97, 145–156.
- Chung, C.-J.F., Fabbri, A.G., 2003. Validation of spatial prediction models for landslide hazard mapping. *Nat. Hazards* 30 (3), 451–472.
- Conoscenti, C., Agnesi, V., Angileri, S., Cappadonia, C., Rotigliano, E., Märker, M., 2013. A GIS-based approach for gully erosion susceptibility modelling: a test in sicily, Italy. *Environ. Earth Sci.* 70 (3), 1179–1195.
- Conoscenti, C., Ciaccio, M., Caraballo-Arias, N.A., Gómez-Gutiérrez, Á., Rotigliano, E., Agnesi, V., 2015. Assessment of susceptibility to earth-flow landslide using logistic regression and multivariate adaptive regression splines: a case of the Belice river basin (western Sicily, Italy). *Geomorphology* 242, 49–64.
- Copons, R., Vilaplana, J.M., 2008. Rockfall susceptibility zoning at a large scale: From geomorphological inventory to preliminary land use planning. *Eng. Geol.* 102 (3–4), 142–151.
- Domeneghetti, A., Vorogushyn, S., Castellarin, A., Merz, B., Brath, A., 2013. Probabilistic flood hazard mapping: effects of uncertain boundary conditions. *Hydrol. Earth Syst. Sci.* 17 (8), 3127–3140.
- Farr, T.G., Rosen, P.A., Caro, E., Crippen, R., Duren, R., Hensley, S., Kobrick, M., Paller, M., Rodriguez, E., Roth, L., et al., 2007. The shuttle radar topography mission. *Rev. Geophys.* 45 (2).
- Funk, C., Peterson, P., Landsfeld, M., Pedreros, D., Verdin, J., Shukla, S., Husak, G., Rowland, J., Harrison, L., Hoell, A., Michaelson, J., 2015. The climate hazards infrared precipitation with stations—a new environmental record for monitoring extremes. *Sci. Data* 2 (150066).
- Gerzsenyi, D., 2021. FRMOD, a python tool for statistical landslide susceptibility assessment. *Adv. Cartogr. GISci. ICA* 3.
- Goetz, J., Brenning, A., Petschko, H., Leopold, P., 2015. Evaluating machine learning and statistical prediction techniques for landslide susceptibility modeling. *Comput. Geosci.* 81, 1–11.
- Goetz, J.N., Guthrie, R.H., Brenning, A., 2011. Integrating physical and empirical landslide susceptibility models using generalized additive models. *Geomorphology* 129 (3–4), 376–386.
- Guzzetti, F., Reichenbach, P., Cardinali, M., Galli, M., Ardizzone, F., 2005. Probabilistic landslide hazard assessment at the basin scale. *Geomorphology* 72 (1–4), 272–299.
- Hijmans, R.J., Cameron, S.E., Parra, J.L., Jones, P.G., Jarvis, A., 2005. Very high resolution interpolated climate surfaces for global land areas. *Int. J. Climatol. A J. R. Meteorol. Soc.* 25 (15), 1965–1978.
- Hong, H., Liu, J., Zhu, A.-X., 2020. Modeling landslide susceptibility using LogitBoost alternating decision trees and forest by penalizing attributes with the bagging ensemble. *Sci. Total Environ.* 718, 137231.
- Ilmy, H.F., Darminto, M.R., Widodo, A., 2021. Application of machine learning on google earth engine to produce landslide susceptibility mapping (case study: Pacitan). In: *IOP Conference Series: Earth and Environmental Science*, Vol. 731. (1), IOP Publishing, 012028.
- James, T., Schillaci, C., Lipani, A., 2021. Convolutional neural networks for water segmentation using sentinel-2 red, green, blue (RGB) composites and derived spectral indices. *Int. J. Remote Sens.* 42 (14), 5338–5365.
- Klügel, J.-U., 2008. Seismic hazard analysis—Quo vadis? *Earth-Sci. Rev.* 88 (1–2), 1–32.
- Lagomarsino, D., Tofani, V., Segoni, S., Catani, F., Casagli, N., 2017. A tool for classification and regression using random forest methodology: Applications to landslide susceptibility mapping and soil thickness modeling. *Environ. Model. Assess.* 22 (3), 201–214.
- Leoni, G., Barchiesi, F., Catallo, F., Dramis, F., Fubelli, G., Lucifora, S., Mattei, M., Pezzo, G., Puglisi, C., 2009. GIS methodology to assess landslide susceptibility: application to a river catchment of central Italy. *J. Maps* 5 (1), 87–93.
- Lin, Q., Lima, P., Steger, S., Glade, T., Jiang, T., Zhang, J., Liu, T., Wang, Y., 2021. National-scale data-driven rainfall induced landslide susceptibility mapping for China by accounting for incomplete landslide data. *Geosci. Front.* 12 (6), 101248.
- Lombardo, L., Cama, M., Conoscenti, C., Märker, M., Rotigliano, E., 2015. Binary logistic regression versus stochastic gradient boosted decision trees in assessing landslide susceptibility for multiple-occurring landslide events: application to the 2009 storm event in Messina (Sicily, southern Italy). *Nat. Hazards* 79 (3), 1621–1648.
- Lombardo, L., Cama, M., Märker, M., Rotigliano, E., 2014. A test of transferability for landslides susceptibility models under extreme climatic events: application to the Messina 2009 disaster. *Nat. Hazards* 74 (3), 1951–1989.
- Lombardo, L., Mai, P.M., 2018. Presenting logistic regression-based landslide susceptibility results. *Eng. Geol.* 244, 14–24.
- Lombardo, L., Opitz, T., Ardizzone, F., Guzzetti, F., Huser, R., 2020a. Space-time landslide predictive modelling. *Earth-Sci. Rev.* 103318.
- Lombardo, L., Saia, S., Schillaci, C., Mai, P.M., Huser, R., 2018. Modeling soil organic carbon with quantile regression: Dissecting predictors' effects on carbon stocks. *Geoderma* 318, 148–159.
- Lombardo, L., Tanyas, H., Huser, R., Guzzetti, F., Castro-Camilo, D., 2021. Landslide size matters: A new data-driven, spatial prototype. *Eng. Geol.* 293, 106288.
- Lombardo, L., Tanyas, H., Nicu, I.C., 2020b. Spatial modeling of multi-hazard threat to cultural heritage sites. *Eng. Geol.* 105776.
- Naghibi, S.A., Hashemi, H., Pradhan, B., 2021. APG: A novel python-based ArcGIS toolbox to generate absence-datasets for geospatial studies. *Geosci. Front.* 12 (6), 101232.
- Najafi, Z., Pourghasemi, H.R., Ghanbarian, G., Fallah Shamsi, S.R., 2020. Land-subidence susceptibility zonation using remote sensing, GIS, and probability models in a Google earth engine platform. *Environ. Earth Sci.* 79 (21), 1–16.
- Nandi, A., Shakoor, A., 2010. A GIS-based landslide susceptibility evaluation using bivariate and multivariate statistical analyses. *Eng. Geol.* 110 (1–2), 11–20.
- Neteler, M., Mitasova, H., 2013. Open Source GIS: A GRASS GIS Approach, Vol. 689. Springer Science & Business Media.
- Nicu, I.C., Lombardo, L., Rubensdotter, L., 2021. Preliminary assessment of thaw slump hazard, hazard to arctic cultural heritage in Nordenskiöld land, Svalbard. *Landslides* 18 (8), 2935–2947.
- Rahmati, O., Kornejady, A., Samadi, M., Deo, R.C., Conoscenti, C., Lombardo, L., Dayal, K., Taghizadeh-Mehrjardi, R., Pourghasemi, H.R., Kumar, S., et al., 2019. PMT: New analytical framework for automated evaluation of geo-environmental modelling approaches. *Sci. Total Environ.* 664, 296–311.

- Scheip, C.M., Wegmann, K.W., 2021. HazMapper: a global open-source natural hazard mapping application in Google earth engine. *Nat. Hazards Earth Syst. Sci.* 21 (5), 1495–1511.
- Schratz, P., Muenchow, J., Iturritxa, E., Richter, J., Brenning, A., 2019. Hyperparameter tuning and performance assessment of statistical and machine-learning algorithms using spatial data. *Ecol. Model.* 406, 109–120.
- Seydi, S.T., Akhoondzadeh, M., Amani, M., Mahdavi, S., 2021. Wildfire damage assessment over Australia using sentinel-2 imagery and MODIS land cover product within the google earth engine cloud platform. *Remote Sens.* 13 (2), 220.
- Srb, P., Petru, M., Kulhavy, P., 2017. Numerical simulation of flood barriers. In: *EPJ Web of Conferences*, Vol. 143. EDP Sciences, p. 02115.
- Steger, S., Brenning, A., Bell, R., Petschko, H., Glade, T., 2016. Exploring discrepancies between quantitative validation results and the geomorphic plausibility of statistical landslide susceptibility maps. *Geomorphology* 262, 8–23.
- Taalab, K., Cheng, T., Zhang, Y., 2018. Mapping landslide susceptibility and types using random forest. *Big Earth Data* 2 (2), 159–178.
- Titti, G., Lombardo, L., 2022. giactitti/SRT: SRT v1.0. Zenodo.
- Titti, G., Sarretta, A., Lombardo, L., Crema, S., Pasuto, A., Borgatti, L., 2022. Mapping susceptibility with open-source tools: a new plugin for QGIS. *Front. Earth Sci.* 229.
- Titti, G., van Westen, C., Borgatti, L., Pasuto, A., Lombardo, L., 2021. When enough is really enough? On the minimum number of landslides to build reliable susceptibility models. *Geosciences* 11 (11), 469.
- Tonini, M., D'Andrea, M., Biondi, G., Degli Esposti, S., Trucchia, A., Fiorucci, P., 2020. A machine learning-based approach for wildfire susceptibility mapping. the case study of the Liguria region in Italy. *Geosciences* 10 (3), 105.
- Wang, N., Cheng, W., Marconcini, M., Bachofer, F., Liu, C., Xiong, J., Lombardo, L., 2022. Space-time susceptibility modeling of hydro-morphological processes at the Chinese national scale. *Eng. Geol.* 301, 106586.
- Wang, N., Lombardo, L., Gariano, S.L., Cheng, W., Liu, C., Xiong, J., Wang, R., 2021. Using satellite rainfall products to assess the triggering conditions for hydro-morphological processes in different geomorphological settings in China. *Int. J. Appl. Earth Obs. Geoinf.* 102, 102350.